JOURNAL OF APPLIED ELECTROCHEMISTRY 21 (1991) 597–605

Dependence of performance of solid polymer electrolyte fuel cells with low platinum loading on morphologic characteristics of the electrodes

E. A. TICIANELLI*, J. G. BEERY, SUPRAMANIAM SRINIVASAN‡

Los Alamos National Laboratory, Los Alamos, New Mexico 87545, USA

Received 4 July 1989; revised 2 August 1989

This paper describes the results of transmission electron microscopic, scanning electron microscopic and/or Rutherford backscattering spectroscopic analyses of platinum electrocatalysts supported on carbon, and of low catalyst loading gas-diffusion electrodes used in proton-exchange-membrane (PEM) fuel cells. We looked for correlations between the performance of PEM fuel cells and the morphology of low-catalyst-loading electrodes, taking into account the thickness of the catalyst layers, the crystallite sizes of the platinum electrocatalyst supported on carbon and the increased Pt catalyst content near the front of the electrodes. We reached the conclusion that the use of electrodes with thin catalyst layers (made by using platinum on carbon electrocatalysts with a high Pt/C weight ratio) and with more platinum localized near the front surface had the effect of diminishing the overpotentials in PEM fuel cells.

1. Introduction

One of the principal objectives of the fuel cell programme at Los Alamos is to develop proton-exchange-membrane (PEM) fuel cell systems with electrodes containing a platinum loading one-tenth or less of the loading in state-of-the-art PEM fuel cells. Our approach was to impregnate a proton conductor, such as Nafion (registered trademark of Du-Pont, Inc.), into a porous gas-diffusion electrode which contains only $0.4\,mg\,cm^{-2}$ platinum (the platinum loading in state-of-the-art PEM fuel cells is $4\,mg\,cm^{-2}$) and use the impregnated electrode in the fabrication of membrane and electrode assemblies for PEM half- or single-cells. By using such electrodes in half- [1] and single- [2] PEM fuel cells, we demonstrated that the same level of performance could be attained as in PEM cells with 10 times the noble metal loading. We also showed that the electrochemically active surface area for the low-platinum-loading electrode with Nafion impregnation nearly equalled that of the high-platinum-loading electrode and was more than 10 times greater than for the low-platinum-loading electrode without Nafion impregnation. The latter finding was demonstrated by comparing the performances of PEM fuel cells containing low-platinum-loading electrodes with and without Nafion impregnation. We concluded that the *modus operandi* of the Nafion-impregnated electrodes is by an extension of the three-dimensional reaction zone in the porous gas-diffusion electrode. Following impregnation by the ionomer, the electrochemically active area of such a membrane-electrode assembly is nearly the same as that of the same low-platinum-loading electrode in contact with a liquid electrolyte such as phosphoric acid or potassium hydroxide.

Recently high power densities have been reported for PEM fuel cells with high-platinum-loading electrodes ($> 1\,W\,cm^{-2}$; maximum power densities for advanced phosphoric acid fuel cells $= 0.2\,W\,cm^{-2}$). In order to approach such power densities with low-platinum-loading electrodes, we found it necessary to modify the electrode structure and operating conditions. Results of such investigations have been reported in two papers [3, 4]. These studies focused on the optimization of cell performance based on the following parameters: (1) the amount of Nafion impregnated into the electrodes; (2) the conditions for hot-pressing electrodes to the membrane; (3) the humidification of reactant gases for attaining optimum water-management conditions in the cells; (4) the effect of polytetrafluoroethylene (PTFE) content in the electrodes; (5) the effect of temperature and pressure; (6) the effect of the thickness of the catalyst layer; and (7) the effect of localization of platinum near the front surface of the electrode. The cell performance was determined by measurements of cell potential versus current density (at constant P and T), cell potential as a function of oxygen pressure (at constant i and T), cell potential versus time (at constant i, P and T) and cyclic voltammetry. The optimum cell performance was obtained by (1) using Prototech, Inc. (Newton Highlands, Massachusetts, USA), carbon cloth electrodes ($0.4\,mg\ Pt\,cm^{-2}$), which contained

*Present address: Instituto de Fisica e Quimica de S. Carlos—USP, Caixa Postal 369-CEP, 13560 Saõ Carlos, Saõ Paulo, Brazil.
‡ Present address: Center for Electrochemical Systems and Hydrogen Research, TEES, TAMUS, College Station, Texas 77843-3577, USA.

0021-891X/91 $03.00 + .12

20 wt % Pt/C electrocatalysts and on which was sputtered 0.05 mg cm^{-2} Pt on the front surface (corresponding to 50 nm on a smooth surface); (2) impregnation of the electrodes with 0.6 mg cm^{-2} Nafion (dry weight); (3) operating at a cell temperature of 80° C and a pressure of 3 atm hydrogen and 5 atm oxygen or air; and (4) humidifying the gases at a temperature higher than the cell temperature (by 10–15° C for H_2 and by 5° C for air or oxygen). These investigations of correlations between the performance of porous electrodes and their structure, or operating conditions, were based only on published concepts and models of porous gas-diffusion electrodes [5]. For a detailed analysis of the dependence of fuel cell performance on the morphology of porous diffusion electrodes, it is necessary to use non-electrochemical techniques such as transmission electron microscopy, scanning electron microscopy and Rutherford backscattering spectroscopy, as presented in this paper.

Transmission electron microscopy (TEM) has often been used to examine fuel cell components [6–8], mainly to characterize carbon-supported platinum catalyst powders used in the fabrication of electrodes. One problem with this technique lies in the preparation of samples for electron microscopy. It is difficult to maintain the physical integrity of the specimen required to correlate the physical structure of the gas-diffusion electrode with the performance of fuel cells. Scanning electron microscopy (SEM) working in the reflection mode may appear adequate for carrying out such analysis, but the resolution of the technique is not sufficient to elucidate the microstructure of the electrode, which determines the kinetics of the electrochemical reactions. Such problems with the two electron microscopic techniques are the reason why only a few attempts [8, 9] have been made to examine the microstructure of porous gas-diffusion electrodes. In spite of these facts, TEM shows promise for analysing carbon-supported electrocatalyst powders. Rutherford backscattering spectroscopy (RBS) is another technique that has been used for the examination of gas-diffusion electrodes [10]. RBS does not provide information about the microstructure (porosity, particle sizes, etc.), but it does provide atomic concentration ratios as a function of depth, assuming the physical density is known. Porous gas-diffusion electrodes are particularly suitable for RBS analysis because they are usually composed of a high atomic number (Z) element, Pt, distributed in a low-Z element matrix containing C, O and F. Consequently, the scattered α-particles are at a higher energy for Pt than for the low-Z elements. In addition, the scattering cross-sections are proportional to Z^2, so the platinum scattering is enchanced relative to the carbon scattering.

This paper describes the results of TEM, SEM and RBS analysis of supported Pt on C electrocatalysts and low-catalyst-loading porous gas-diffusion electrodes used in the studies previously described for PEM fuel cells. For purposes of analysing the dependence of fuel cell performance on the morphology of the electrodes, some electrochemical results obtained in single-cell testing are also included in this paper.

2. Experimental details

2.1. *Materials*

Platinum on carbon electrocatalysts were custom-made by Prototech, Inc., containing 10, 20 and 40 wt % Pt/C. Such powders were also used by Prototech, Inc., for the preparation of low-catalyst-loading gas-diffusion electrodes, all with 0.4 mg Pt cm^{-2}. These electrodes were composed of a Teflon (registered trademark of du-Pont, Inc.) carbon cloth backing, a diffusion layer (that partially penetrates into the carbon cloth) containing 50 wt % PTFE and a catalyst layer with 40 wt % and 60 wt % Pt/C electrocatalyst. Sputtering a thin layer of Pt on top of the catalyst layer of the electrodes, corresponding to an extra Pt loading of 0.05 mg cm^{-2}, was accomplished using a planar radio-frequency sputtering chamber.

Before the membrane and electrode (M&E) assembly preparation, the catalyst side of the porous gas-diffusion electrode samples were coated with a thin film of Nafion by brushing a 5 wt % Nafion in 85 wt % isopropanol/water solution (Nafion 1100 solution provided by Solution Technology, Inc.). The solvent was evaporated at room temperature, after which the samples were dried at 70° C under vacuum for 1 h.

M&E assemblies were prepared by first placing a pair of Nafion-impregnated electrodes on both sides of a Nafion membrane (Nafion 117) and in between two thin stainless steel plates (0.5 mm thick); the assembly was then inserted between the two platens of a hot-press (Carver, type C) preheated to 95–100° C; the temperature of the hot-press was subsequently raised to 125–130° C, at which time a pressure of 50–60 atm was applied on the sample for 90 s. The M&E assemblies were removed from the hot-press just after this treatment and allowed to cool under ambient conditions.

2.2. *Electrochemical experiments*

The electrochemical experiments were carried out in single-cell test stations as described in detail in [3]. The operating temperature of the electrochemical cell was 80° C; humidification of oxygen was carried out by bubbling through water preheated to 85° C; the same apparatus was used for hydrogen, but the water temperature was 90–95° C. The pressure of reactant gases was 3 atm for hydrogen and 5 atm for oxygen.

2.3. *SEM analysis*

Although some investigations of the catalyst layer of the porous gas diffusion electrodes were made, the SEM analysis was also used to examine cross-sections of the M&E assemblies. Sample of the M&E assemblies for such analyses were sliced, with a razor blade, from a larger piece previously cooled in liquid nitrogen

(77 K). This procedure was found to be adequate to minimize compression and damage to several layers of the M&E assemblies, including the diffusion and catalyst layers of the electrodes. A Philips Model 505 SEM was used. The instrument was operated at a beam energy of 30 keV.

2.4. *TEM analysis*

The TEM analysis was conducted on the supported platinum on carbon electrocatalysts powders and on fragments of catalyst layers of porous gas-diffusion electrodes. We dispersed the powders in ether, using an ultrasonic bath, and then mounted them on standard copper TEM grids. We collected fragments of the catalyst layer of electrodes on top of the copper grid by scraping a precooled sample (liquid nitrogen) with a razor blade. As observed in previous work [6] analysing porous gas-diffusion electrodes, only the outer fringes of the fragments could be observed in TEM experiments. A Philips model EM400T TEM was operated at an acceleration voltage of 120 kV in bright-field illumination. Direct magnification ranged from 60 000 to 220 000 ×. Generally, the negatives of the photographs were enlarged 2.4 ×, which allowed an increase in virtual magnification up to 530 000 ×.

2.5. *RBS analysis*

The different kinds of porous gas-diffusion electrodes described in this work were subjected to RBS analysis. Samples consisted of discs of the materials (diameter about 0.6 cm) mounted on aluminium holders with the catalyst layers perpendicular to the incident ionic beams. RBS experiments were performed at the ion-beam facility of Los Alamos National Laboratory according to a conventional arrangement, as described in [10–12]. The low-energy (2 MeV) α-particle analysis provides accurate atom percentage ratios, and the 3 MeV proton beam penetrates more deeply to give depth profile information.

3. Results

3.1. *Electrochemical experiments*

When the fuel cell operates at high current densities, most of the current tends to be generated near the front surface of the electrocatalyst layer of the electrode [5]. Thus, localization of the electrocatalyst near the front surface will be most beneficial. In addition, to minimize the mass transport and ohmic limitations within the active layer that predominate at high current densities, it may be desirable to have a thin electrocatalyst layer in the electrode.

As discussed previously [4], we chose three methods of implementing changes in the electrode structures in order to have electrodes with thin electrocatalyst layers and with platinum concentrated near the front surface. In the first method electrodes were used with 20 and 40 wt % Pt/C, but practically the same

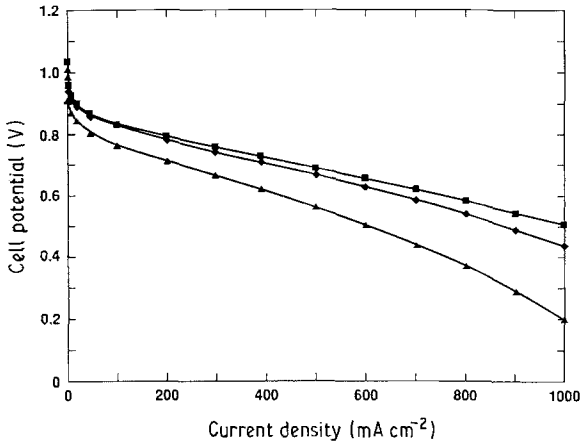

Fig. 1. Effect on an increase in weight percentage Pt/C of supported electrocatalysts in electrodes (0.4 mg cm^{-2} Pt) on H_2/air single-cell performance at 80° C and 0.6 atm. (▲) 10, (◆) 20 and (■) 40 wt % Pt/C.

platinum loading (0.4 mg cm^{-2}) was maintained as in the conventional electrodes, with 10 wt % Pt/C. Thus, the thickness of the active layers decreased in the electrodes with high Pt/C ratio. In the second approach a thin layer of platinum was sputter-deposited (0.05 mg cm^{-2}) on the standard electrodes containing 10 wt % Pt/C (this corresponds to a thickness of 50 nm on a smooth surface). A modification based on the combination of the two methods was to deposit a thin film of platinum (0.05 mg cm^{-2}) on the porous gas-diffusion electrodes prepared with a higher Pt/C ratio (20 and 40 wt %). The total platinum content in these electrodes was less than 0.5 mg cm^{-2}.

Using electrodes with higher Pt/C ratio effected a significant improvement in the performance of the cell potential versus current density (Fig. 1). Sputtering a thin film of platinum on the standard electrode (10 wt % Pt/C) also improved significantly the performance of the cell (Fig. 2), resulting in a reduction in the overpotentials at current densities up to 1 A cm^{-2}. In addition, the sputtered platinum increased the performance of the electrode with 20 wt % Pt/C (Figs 1 and 2) by reducing activation, as well as other

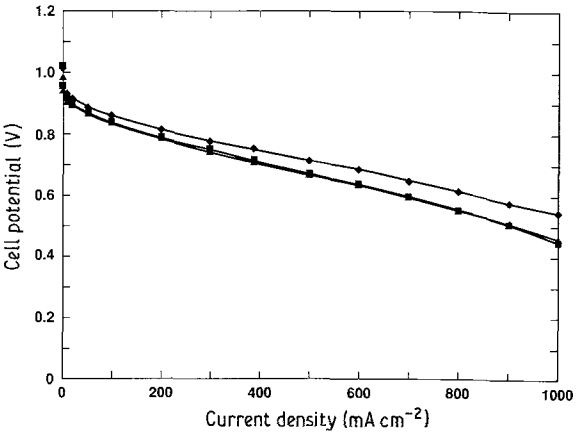

Fig. 2. Effect of increasing platinum loading near the front surface of the electrode by sputtering a 50 nm film of platinum on the electrodes with increasing weight percentage Pt/C in supported electrocatalyst on H_2/air single-cell performance at 80° C and 0.6 atm. (▲) 10, (◆) 20 and (■) 40 wt % Pt/C. Total platinum loadings were 0.45 mg cm^{-2}.

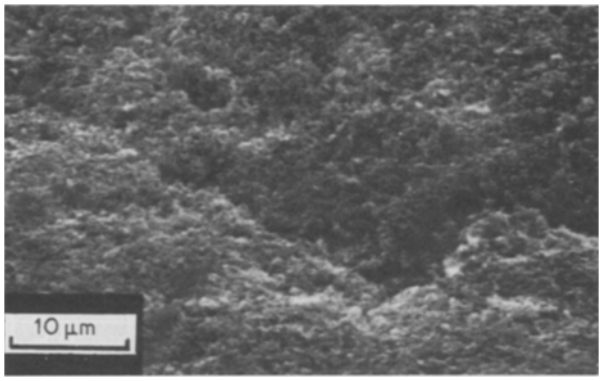

Fig. 3. SEM micrograph of the catalyst layer of the 20 wt % Pt/C electrode with a sputtered layer of Pt (50 nm).

losses in the cell. The overall effect of sputtering was less pronounced in the 20 wt % Pt/C than in the 10 wt % Pt/C. Finally, the 40 wt % Pt/C electrodes with and without the sputtered platinum showed nearly the same level of performance as that of the 20 wt % Pt/C electrodes (Figs 1 and 2).

3.2. *SEM analysis*

Fig. 3 is a SEM photograph of the top catalyst layer of an electrode with 20 wt % Pt/C on to which a sputtered layer of platinum was incorporated (corresponding to 50 nm on a smooth surface or 0.05 mg Pt cm^{-2} in the porous gas-diffusion electrode). The figure illustrates a general observation that such a small amount of sputtered platinum does not introduce any visible change to the microstructure of the electrode. When the resolution of the SEM analysis is taken into account, the sputtered platinum seems to be completely dispersed over the high surface of the Pt/C/PTFE support.

The general features of the cross-section of the M&E assemblies are illustrated in Fig. 4 from a SEM examination of the 20 wt % Pt/C + 0.05 mg cm^{-2} of sputtered platinum electrodes hot-pressed on both sides of the membrane. The three components of the M&E assembly are easily distinguishable in the photograph. It is important to note the very good adhesion of the electrodes to the membrane; this was observed only with the optimized hot-pressing conditions described in [2].

Other interesting features related to the porous gas-diffusion electrode structures also appear in Fig. 4. The carbon cloth substrate is the most pre-eminent component of the electrode structure, defining the overall thickness, and to some extent the open channels for the reactant gas to reach the catalyst layer located adjacent to the membrane. There is no distinction in the appearance of the catalyst and the diffusion layers; thus, it may be concluded that the SEM analysis does not identify the boundary between the two layers or the degree of intermixing between the two. However, according to the methodology for the electrode preparation (by Prototech, Inc.), the open spaces of the carbon cloth were first filled with the diffusion layer constituents on to which the catalyst layer was deposited.

Fig. 4. SEM micrograph of cross-section of M&E assembly of the 20 wt % Pt/C electrode with sputtered layer of Pt (50 nm).

3.3. *TEM analysis*

TEM photographs of the platinum crystallites supported on carbon catalysts, 10, 20 and 40 wt % Pt/C used in the electrode preparation, appear as Figs 5–7. A similar photograph of uncatalysed carbon (Vulcan XC-72 supplied by Cabot Corporation, Newton Highlands, Massachusetts, USA) appears as Fig. 8. Comparing Figs 5–7 with Fig. 8 shows that the platinum electrocatalyst appears in the photographs as dark spots with the sizes depending on the Pt/C weight ratio; the higher the ratio, the bigger the average particle size. In all three cases the platinum crystallites seem to be homogeneously dispersed and to adhere to the carbon particles. The dark-fields in the photographs are probably due to the existence of thicker regions of the analysed powders, which makes transmission of the electrons through those regions of the sample difficult.

The TEM photographs were further analysed to estimate the distribution of platinum particle sizes for all three types of platinum on carbon catalysts. This

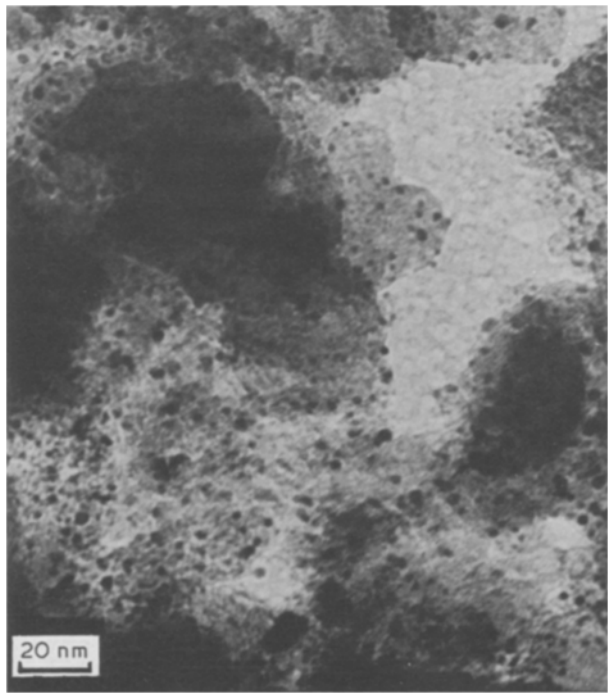

Fig. 5. TEM micrograph of 10 wt % Pt/C electrocatalyst powder (Prototech). Vulcan XC-72 carbon support.

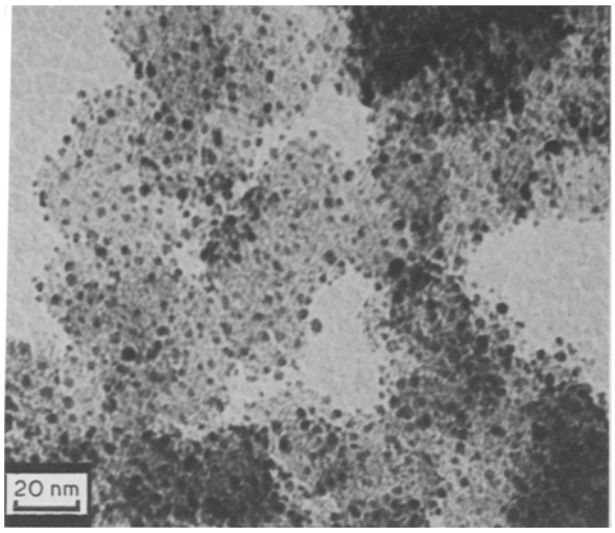

Fig. 6. TEM micrograph of 20 wt % Pt/C electrocatalyst powder (Prototech). Vulcan XC-72 carbon support.

was done by counting and measuring the average diameter of 300 particles, randomly distributed in the area covered by the photograph. The reproducibility of the method was checked by repeating the procedure twice for the 20 wt % Pt/C catalyst; two independent measurements resulted in diameters within 2% of each other. The results of such analysis are presented in the bar charts of Figs 9–11.

In the 10 wt % Pt/C electrocatalysts, most of the platinum particles had diameters ranging from 1.2 to 4.5 nm. Of the catalysts, 80% had diameters between 1.2 and 2.5 nm whereas the average diameter (d) of particles, calculated using

$$d = \frac{\sum\% \times \text{particle size}}{100}$$

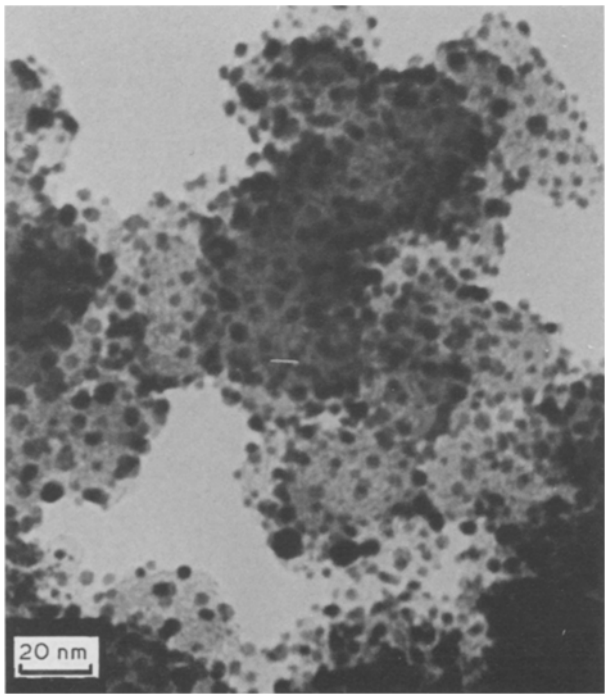

Fig. 7. TEM micrograph of 40 wt % Pt/C electrocatalyst powder (Prototech). Vulcan XC-72 carbon support.

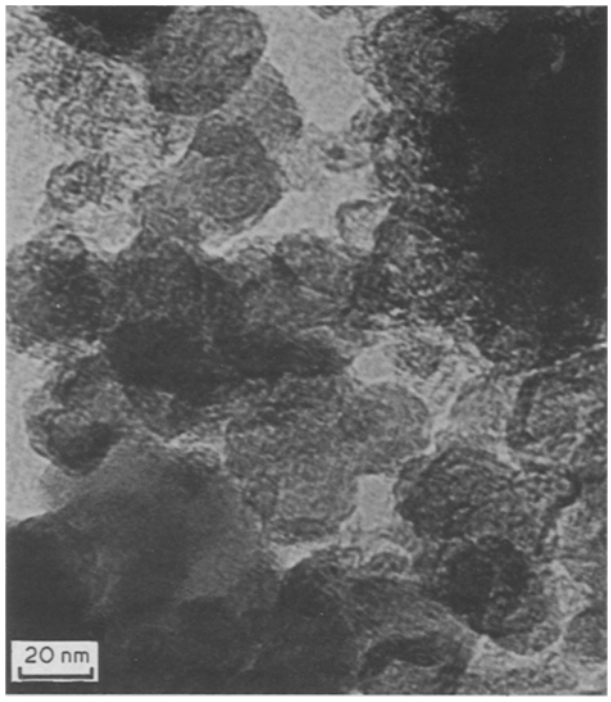

Fig. 8. TEM micrograph of Vulcan XC-72 carbon support.

was 2.2 nm. The platinum particles in the 20 wt % Pt/C had diameters between 1.2 and 6.2 nm, and 60% had diameters between 1.8 and 3.2 nm. The average diameter (d) was 2.9 nm. In the 40 wt % Pt/C, diameters ranged between 1.2 and 7.5 nm, 70% were between 1.8 and 4.0 nm, and d = 3.9 nm.

The TEM photographs of fragments of the catalyst layer in 20 wt % Pt/C electrodes without sputtered platinum appear in Fig. 12. It was generally observed during the analysis of the electrode with 20 wt % Pt/C catalyst (Fig. 12) that most of the carbon particles containing the platinum crystallites were agglomerated, probably bonded by the PTFE ligand used as a wet-proofing and bonding agent. However, there was no direct evidence of PTFE in any of the fields analysed. The absence of PTFE is in agreement with the results of [6]*. The platinum crystallites in this electrode had approximately the same particle sizes as the 20 wt % Pt/C electrocatalyst powder shown in Fig. 6.

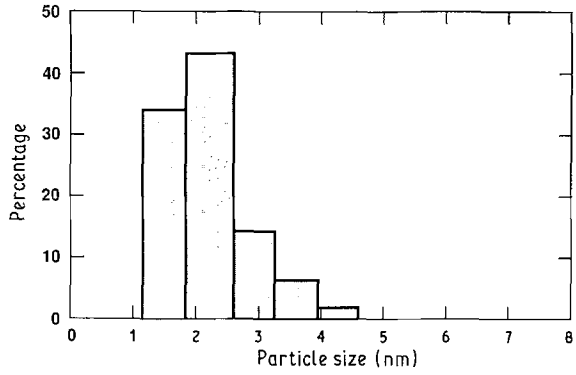

Fig. 9. Distribution of particle sizes in 10 wt % Pt/C electrocatalyst. Particle sizes are average diameters.

*Presumably, the thin PTFE films melt from the electron-beam heating in the TEM.

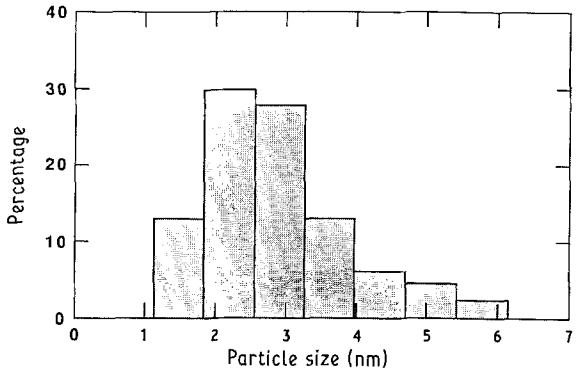

Fig. 10. Distribution of particle sizes in 20 wt % Pt/C electrocatalyst. Particle sizes are average diameters.

The effect of incorporating the sputtered platinum in the 20 wt % Pt/C electrode is illustrated in the TEM photograph (Fig. 13). The agglomeration of the carbon support can be observed more easily in Fig. 13, because of the higher contrast brought about by the sputtering. The sputtered catalyst appears to cover the whole agglomeration. The catalyst is finely dispersed and seems to conform to the morphology of the carbon support particles.

3.4. *RBS analysis*

In Figs 14–16 the RBS spectra (α-particles) of the 10, 20 and 40 wt % Pt/C electrodes appear. The full curves correspond to the computer-generated plots, obtained by fitting the experimental data and using a multilayer model [13]. The most prominent edges appearing in the spectra are those for platinum (1.8 MeV) and carbon (0.5 MeV). Less prominent is the edge of fluorine (from PTFE), which is about 0.8 MeV and is highlighted in Fig. 14 by the simulated curve.

The depth of penetration of the α-particles in the catalyst layers of the porous gas-diffusion electrodes has been estimated previously [12] to be in the range 6–8 μm. Although some non-homogeneity can be found within this depth of the catalyst layer, some useful information can be obtained by analysing the RBS carbon spectra. According to the theoretical model [13], the relative height of the platinum edge to the carbon edge gives information about the Pt/C atomic ratio for each electrode and, consequently,

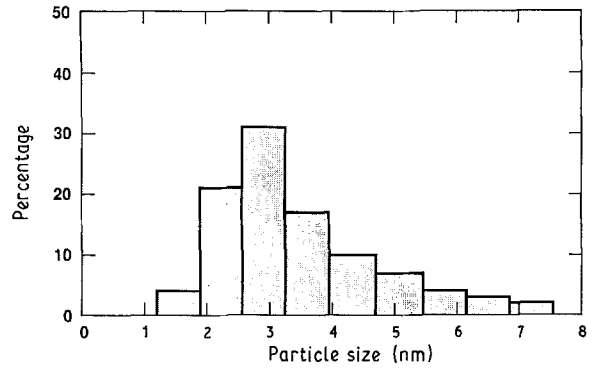

Fig. 11. Distribution of particle sizes in 40 wt % Pt/C electrocatalyst. Particle sizes are average diameters.

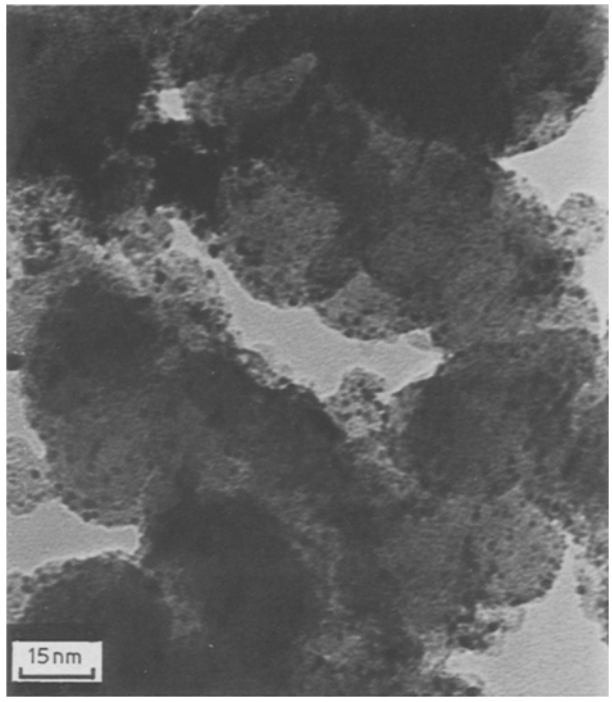

Fig. 12. TEM micrograph of sintered catalyst layer of 20 wt % Pt/C electrode.

about the platinum concentration on the catalyst layers of the electrodes. Using the spectra of Figs 14–16, the resulting values were in the ratio of 1 : 2.4 : 4 for the electrodes with 10, 20 and 40 wt % Pt/C catalyst, respectively. The small signal for the fluorine atoms does not permit calculation of the PTFE content of the electrodes.

The spectra obtained by using the proton beams in the RBS experiments are illustrated in Figs 17 and 18, for the 20 wt % Pt/C electrodes without (Fig. 17) and with (Fig. 18) the sputtered layer of platinum. In

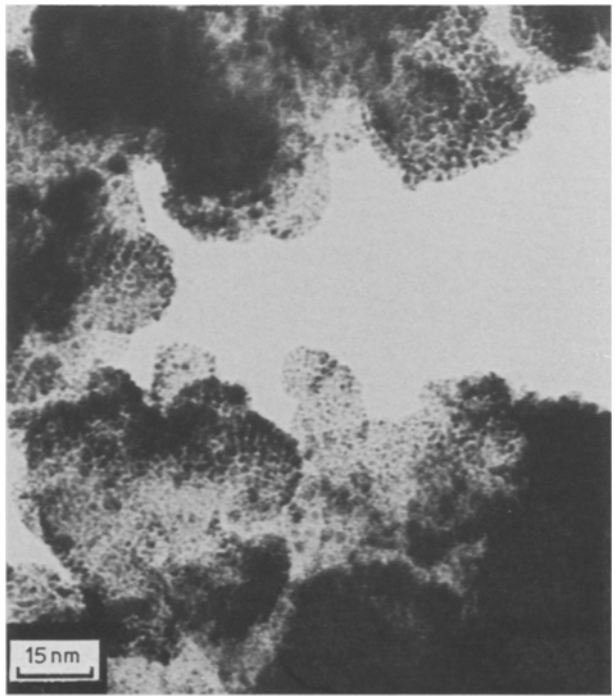

Fig. 13. TEM micrograph of sintered catalyst layer of 20 wt % Pt/C electrode with sputtered layer of Pt (50 nm).

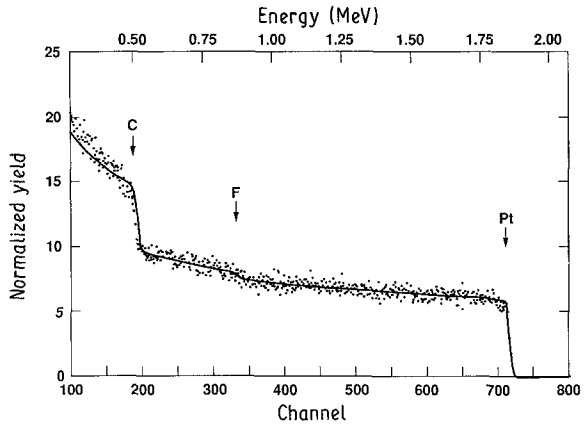

Fig. 14. RBS spectrum of 2 MeV α-particle scattered from a 10 wt % Pt/C catalyst layer electrode, (· · ·) data, (——) computer simulation.

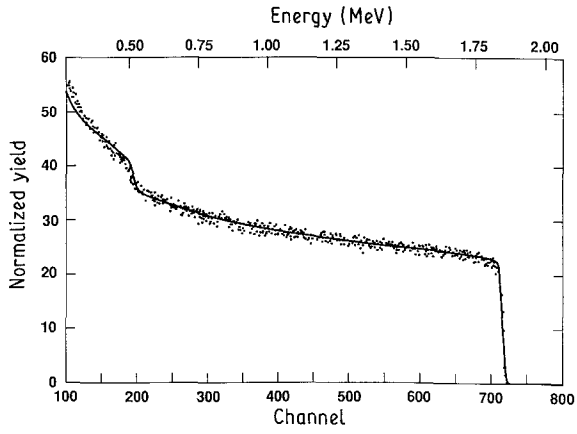

Fig. 16. RBS spectrum of 2 MeV α-particles scattered from a 40 wt % Pt/C catalyst layer electrode, (· · ·) data, (——) computer simulation.

Fig. 17 the peaks in the spectrum are for platinum (3.0 MeV), fluorine (2.5 MeV), oxygen (2.4 MeV) and carbon (2.2 MeV). The sharp peak appearing around 3.0 MeV in the spectrum in Fig. 18 is clearly related to the presence of the sputtered layer of platinum near the electrode surface.

The experimental data obtained by using the proton beam for the RBS analysis were simulated with computer algorithms for interpretation of RBS spectra. A key assumption in the computer code is that the samples are made of a finite number of layers of different thicknesses, each with uniform composition [13]. Using this technique it was determined that the thicknesses of the catalyst layers are 100, 50 and 25 μm for the electrodes with 10, 20 and 40 wt % Pt/C, respectively. This determination is based on the assumption that the total catalyst loading is the same for all three electrodes. In any case the Pt/C atomic ratio in the first 6–8 μm is measured by the RBS to be 0.7, 1.7 and 2.8% for the electrodes with 10, 20 and 40 wt %, respectively. In addition, it was found that the sputter-deposited platinum penetrates only minimally into the electrode structure and is located within a thickness of about 0.5 μm on the front surface of the electrode.

3.5. *Correlation between electrochemical performance of PEM fuel cells and morphological characteristics of the electrodes*

As shown in the TEM and RBS analyses, there were two major observations related to the electrode structures with the three types of platinum on carbon catalysts used for preparation of the catalyst layers. First, TEM showed that the average sizes of platinum crystallites increased as the Pt/C ratio increased from 10 to 20 to 40 wt % Pt/C. Secondly, the RBS analysis confirmed that the platinum loading was roughly in the ratio of 1 : 2 : 4 for the 10, 20 and 40 wt % catalyst mixtures. Table 1 summarizes these results. Since the effective depth of penetration for the Nafion impregnation additive, as obtained by brushing a Nafion solution on to the front surface of the electrode, is about 10 μm, the third column gives the geometrical platinum area in the outer 10 μm of the electrode. For comparision the effective surface areas of platinum as obtained by cyclic voltammetry [4] are also included in the table. These two areas correlate well.

The improvement in the activation region (Fig. 1), which is usually related to an increase in the effective surface area of the electrodes, apparently contradicts the results of the TEM analysis if the total surface area of Pt in the catalyst layer is considered. This apparent

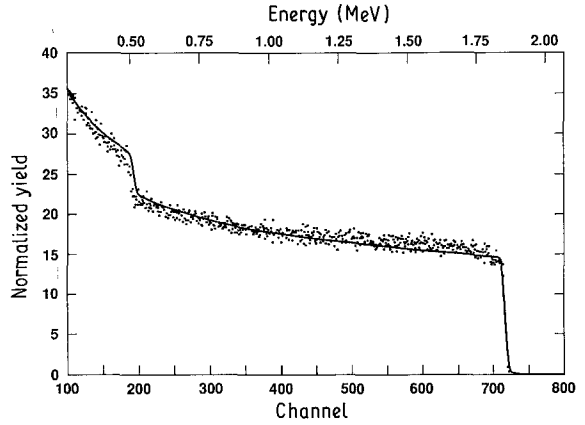

Fig. 15. RBS spectrum of 2 MeV α-particles scattered from a 20 wt % Pt/C catalyst layer electrode, (· · ·) data, (——) computer simulation.

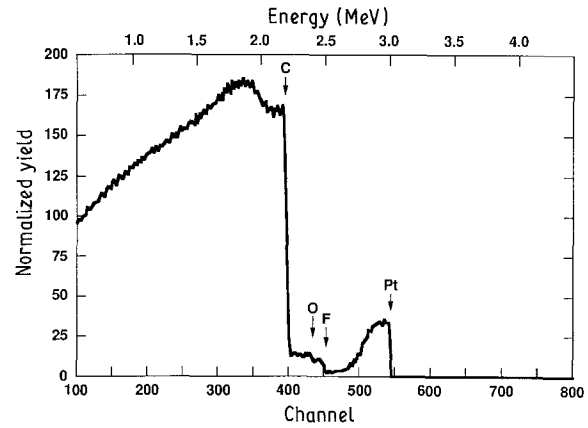

Fig. 17. RBS spectrum of 3 MeV protons scattered from a 20 wt % Pt/C catalyst layer electrode.

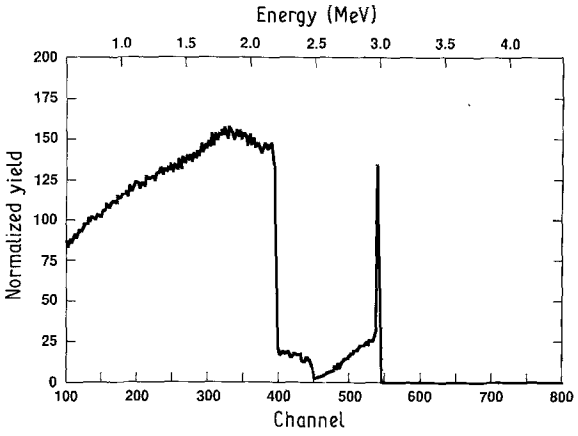

Fig. 18. RBS spectrum of 3 MeV protons scattered from a 20 wt % Pt/C catalyst layer electrode with a sputtered layer of Pt/(50 nm).

contradiction can be resolved if it is considered that the Nafion impregnated into the electrodes penetrates only partially into the structure; that is, within a thickness of about 10 μm [4]. Thus, as the electrode containing a higher weight percentage of Pt/C has a higher concentration of platinum particles near the front surface, the overall result is an effective increase in the active area of the Nafion-impregnated electrode. This phenomenon is supported by the results of the cyclic voltammetric experiments carried out on all of the electrodes (Table 1). The voltammetric charge capacity, determined from the hydrogen adsorption–desorption region on platinum [4], demonstrates clearly an increase for the impregnated electrodes with higher Pt/C concentrations.

The present analysis also refers to the increase of the electrode performance (Fig. 1) with the increase of the Pt active areas (Table 1). The increase in cyclic voltammetric surface area for the electrode with 20 wt % Pt/C compared with the electrode with 10 wt % Pt/C is 33 $cm^2 cm^{-2}$ (geo). This difference significantly improves the performance of the fuel cell (see curves a and b in Fig. 1). On the other hand, the increase in surface area for the electrode with 40 wt % Pt/C compared with that for the electrodes with 20 wt % Pt/C is 24 $cm^2 cm^{-2}$ (geo) but there was no corresponding improvement in the fuel cell performance (see Fig. 1). The reason for this seems to be related to the microstructure of the electrodes with the different weight percentages of Pt/C which were not optimized in terms of the PTFE content. This may have introduced some probelms in the hydrophobic properties and/or microporosity of the electrodes with higher Pt/C weight percentages, especially the 40 wt % Pt/C catalyst. Another possible explanation can be given in terms of a shielding effect of the diffusional fields of neighbouring platinum particles, which is more severe with the electrode containing a higher weight percentage of Pt/C [14]. This phenomenon arises if the conventional supported-electrocatalyst, porous gas-diffusion electrodes are considered as an assembly of a large number of ultra-microelectrodes. This may be less severe for the electrodes with 10 and 20 wt % Pt/C, since the average particle sizes are much smaller than the distances separating the neighbouring particles (Figs 5–7).

Table 1. Averaged diameters (d) platinum crystallites in supported electrocatalysts and roughness factor of gas diffusion electrodes as determined by TEM and cyclic voltammetry

Catalyst (wt % Pt/C)	*d (nm)*	*Pt area* ($cm^2 Pt\, cm^{-2}$(geom)) assuming effective depth of 10 μm*	*CV area† ($cm^2 Pt\, cm^{-2}$(geom))*
10	2.2	54	20
20	2.9	82	53
40	3.9	124	77

*Calculated assuming spherical particles for the platinum crystallites and platinum loading in electrodes to a depth of 10 μm.
† Values from [4].

A comparision of the results presented in Figs 1 and 2 shows that sputtering a thin film of platinum on the front surface of the standard electrode (with 10 wt % Pt/C) improved significantly the performance of the cells. There was a reduction in the overpotentials at current densities up to 1 A cm^{-2}. The improvement in the overpotential is explained by a major increase in the electrochemical active surface area of the electrode. As shown by the RBS study, the total amount of extra platinum applied by sputtering, which is located within a thickness of 0.5 μm, is probably completely covered by the Nafion film coating. This extra platinum is responsible for the increase in the surface area. In addition, providing more active sites on the front surface of the electrode had a very positive effect in diminishing internal resistance losses within the catalyst layer.

For the 20 wt % Pt/C electrode the effect of the sputtered layer of platinum was less pronounced than in the previous case. There was an apparent reduction in the activation overpotential, and a negligible effect on the concentration overpotential at current densities up to 1 A cm^{-2}. However, the sputtered layer of platinum (located within 0.5 μm on top of the catalyst layer) provided an increase in the number of active sites near the front surface of the electrode, which was most beneficial in minimizing internal resistance losses within the catalyst layer.

Finally, the 40 wt % Pt/C electrodes with and without the sputtered platinum showed nearly the same performance (Figs 1 and 2). This result is somewhat surprising, considering that the sputtered platinum increases the active area of the electrodes by creating additional active sites. This behaviour is related to the microstructure of the porous gas-diffusion electrocatalyst, as previously discussed.

4. Conclusions

From the results of the present work, the following conclusions can be drawn.

(a) The SEM analysis demonstrates extremely good adhesion of the electrodes to the membrane; this is obtained only with optimized hot-pressing conditions.

(b) The TEM investigations show an increase in platinum crystallite sizes when the Pt/C weight ratio increases in the order 10, 20 and 40 wt % Pt/C electrocatalyst. In addition, we observed that the sputtered platinum, used for localizing the catalyst near the front surface of the electrodes, is deposited as fine particles which appear to cover the carbon support particles, conforming to their surface morphology.

(c) The RBS experiments show that the Pt/C ratio is 1 : 2.4 : 4 for the electrodes with 10, 20 and 40 wt % Pt/C, respectively. In addition, we found that the sputter-deposited platinum penetrates only minimally into the electrode structure and is located within a thickness of about 0.5 μm on the front surface of the electrode.

(d) Use of electrodes with thin catalyst layers (made by using platinum on carbon electrocatalysts with high Pt/C ratio) and with platinum localized near the front surface, had the effect of diminishing activation as well as ohmic losses within catalyst layers of PEM fuel cells.

Acknowledgements

This worked was carried out under the auspices of the US Department of Energy. Edson A. Ticianelli was at Los Alamos National Laboratory on a leave of absence from the University of Saõ Paulo, Saõ Carlos, Brazil. The authors thank Charles R. Derouin, Catherine Mombourquette and Judith Pafford for sputter deposition of platinum on carbon and for assistance in obtaining fuel cell performance data. We acknowledge helpful dicussions with Shimshon Gottesfeld.

References

[1] I. D. Raistrick, in 'Proceedings of the Symposium on Diaphragms, Separators, and Ion Exchange Membranes', (edited by J. W. Zee, R. E. White, K. Kinoshita and H. S. Burney), The Electrochemical Society, Princeton, New Jersey (1986) p. 172.
[2] S. Srinivasan, E. A. Ticianelli, C. R. Derouin and A. Redondo, *J. Power Sources* **22** (1988), 359.
[3] E. A. Ticianelli, C. R. Derouin and S. Srinivasan, *J. Electrochem. Soc.* **135** (1988) 2209.
[4] E. A. Ticianelli, C. R. Derouin and S. Srinivasan, *J. Electroanal. Chem.* **251** (1988) 275.
[5] J. O'M. Bockris and S. Srinivasan, in 'Fuel Cells: Their Electrochemistry', McGraw-Hill, New York (1969) p. 633.
[6] A. Pebler, *J. Electrochem. Soc.* **133** (1986) 9.
[7] A. Honji, T. Mori, K. Tamura and Y. Hishinuma, *J. Electrochem. Soc.* **135** (1988), 355 and references therein.
[8] R. Holze and A. Mass, *J. Appl. Electrochem.* **13** (1983), 549.
[9] J. Aragane, T. Murahashi and T. Odaka, *J. Electrochem. Soc.* **135** (1988), 844.
[10] P. J. Hyde, C. J. Maggiore and S. Srinivasan, *J. Electroanal. Chem.* **168** (1984), 383.
[11] S. Gottesfeld, J. Beery, M. Paffett, M. Hollander and C. Maggiore, *J. Electrochem. Soc.* **133** (1986), 1345.
[12] L. Borodovsky, J. G. Beery and M. Paffett, *Nucl. Instrum. Meth.* **B24/25** (1987), 568.
[13] R. Doolittle, *ibid.* **B9** (1985) 344.
[14] M. Watanabe, H. Sei and P. Stonehart, ECS Extended Abstracts, The Electrochemical Society, Princeton, New Jersey, Vol. 88–1 (1988) p. 732.